Interrogations on the sub-surface strain hardening of grit blasted Ti-6Al-4V alloy

M. Multigner[1,2], E. Frutos[2, 1], C.L. Mera[3], J.Chao[1], J.L. González-Carrasco[1,2, *]

(1) Centro Nacional de Investigaciones Metalúrgicas (CENIM-CSIC), Avda Gregorio del Amo nº 8, 28040 Madrid, Spain
(2) Centro de Investigación Biomédica en Red en Bioingeniería, Biomateriales y Nanomedicina (CIBER-BBN), Madrid, España
(3) AIMEN, C/Relva, 27 A – Torneiros, 36410 Porriño – Pontevedra, Spain

(*) Corresponding author. Tel.: +34 915538900; fax: +34 915347425.
Email address: jlg@cenim.csic.es (J.L. González-Carrasco)

Abstract

In this work we characterize the microstructural changes induced by grit blasting of the Ti6Al4V alloy and their effect on the sub-surface mechanical properties by means of micro- and ultramicro indentations techniques. It has been observed that the severe plastic deformation at the surface produces an increase in roughness. Such deformation, however, does not cause any evident hardening at the sub-surface zone, which contrast with the work hardening observed on blasted cp Ti and austenitic stainless steel 316 L. It is proposed that the different behaviour of the Ti-base alloy is related to its lower strain hardening exponent. The implications of the absence of subsurface hardening on the loss of fatigue strength observed by other authors are analysed.

Keywords: Grit blasting; Ti6Al4V; Mechanical behaviour; Biomaterials

Surface and Coatings Technology 203(14) (2009) 2036–2040

1. Introduction

Ti6Al4V alloy combines mechanical strength, excellent corrosion resistance and good biocompatibility, thus is widely used for the fabrication of a number of orthopaedic and dental implants proven in many experimental and clinical investigations. Efforts to improve their osteointegration, fixation and stability have been addressed by creating a rough surface that increases the surface area available for bone/implant apposition. Particularly important has been the activity for the production of randomly rough surfaces by grit blasting with oxide particles (mostly SiO_2, ZrO_2, or Al_2O_3). Data obtained *in vivo* show that rough surfaces produce better bone fixation than smooth surfaces [1-3] without compromisig the *in vitro* corrosion behaviour [4,5].

The treatment yields a severe plastic deformation of the surface that causes a roughness increase, whose magnitude depends on size, shape, and kinetics energy of the particles reaching the surface. In addition, the treatment induces microstructural changes in a thin zone beneath the blasted surface and leaves compressive residual stresses with a maximum value close to the surface [4,6-9]. It could be expected that this compressive stress state would delay crack initiation and/or slow down crack propagation resulting in an increased fatigue resistance. However, it has been reported that blasting of Ti6Al4V leads to a pronounced decrease of the fatigue strength during either axial or bending fatigue tests [6]. Fatigue limit decreases with increasing roughness; about 20% decrease for fine blasting (Ra ~2 μm) and up to about 40% for samples with coarse blasting (Ra ~ 7 μm) [10]. The loss of fatigue strength for the Ti6Al4V following blasting has been associated to the presence of microcracks at the surface and to the pronounced stress concentration in the vicinity of the particles that remain embedded onto the surface [10].

This fatigue behaviour of grit blasted Ti6Al4V is somewhat puzzling since blasting of cp Ti, causing a similar microstructural damage at the surface, enhances the fatigue properties [4,11]. It is worth noticing that shot peening [12] or fine-particle bombarding [8] of Ti6Al4V alloy, leaving a compressive residual stresses at the surface too, improves the fatigue resistance [12]. Therefore, conclusions about the reasons for the decrease in the fatigue strength of grit blasted Ti6Al4V alloy remain inconclusive.

The benefit of blasting of cp Ti is attributed to the development of residual stresses and work hardening in a shallow depth of about 60 μm beneath the surface [4,11]. Such hardening has been also observed in grit blasted austenitic stainless steel 316 L [13]. However, data in the open literature on the sub-surface hardening of Ti6Al4V following grit blasting are scarce and limited to previous works that indicates the absence of an evident hardening [7,8,14]. In this work we investigate Ti6Al4V disks which surface was modified by a grit blasting process used to get fine roughened surfaces on implant components. The blasted disks were supplied by two different companies that used their own standard practice. Special emphasis is devoted to analyse the microhardness values in the subsurface blasted zone and the relation with the microstructure. Implications of these features on the loss of fatigue strength in the grit blasted Ti6Al4V alloy reported by other authors will be considered.

2. Materials and methods

For this study, blasted disks of Ti6Al4V were supplied by two different sources; BIOMET (Valencia, Spain) and SURGIVAL (Valencia, Spain). Disks have a thickness of 2 mm. They were removed from hot rolled annealed (700ºC/1h) bars of 20 and 25 mm in diameter, respectively. The specimens revealed a biphasic α+β microstructure that is consistent with its chemical composition and thermomechanical treatment. Blasting was performed by the implant manufacturers following their standard procedure to get fine blasted surfaces on commercial implant components. Disks supplied by BIOMET, hereafter BL1 specimens, were grit blasted by using a jet of alumina particles of about 500 μm in diameter, a pressure of about 0,4 MPa, and a working distance of about 80 mm from the nozzle. Blasting lasted for about 30 to 60 s. Specimens supplied by SURGIVAL, hereafter BL2 specimens, were prepared by grit blasting during 30 s with alumina particles of about 750 μm in diameter and a pressure of about 0,3 MPa. The as-blasted specimens were washed with water containing detergent at 75ºC during 5 min and immersed in a solution of HNO_3 at about 50ºC during 15 min. Finally, the specimens were washed with deionised water for 3 min and sonicated with alcohol.

Microstructural characterization of the surface morphology and cross sections of selected specimens was carried out by scanning electron microscopy (SEM), using a JEOL-6500F instrument equipped with a field emission gun (FEG) and coupled with an energy dispersive X-ray (EDX) system for chemical analysis. Quantitative surface roughness was determined with a profilometer Mitutoyo Surftest 401. The measurements were obtained from line profiles along a 4 mm length. The surface roughness was characterized by average surface roughness (R_a) in micrometer at a high sensitivity setting (0.01 μm).

The hardness distribution beneath the surface was measured on cross-sections of blasted specimens previously coated with a relatively thick layer of Cu obtained by electrolytic deposition. This coating preserves the blasted surface during preparation of the cross section but also allows the approach to the blasted interface with the indenter. The Vickers microhardness measurements were performed in a Wilson equipment using the minimum load (98 mN) and 15 s of dwell time. Taken into consideration the relative large scattering associated to the small load and to minimise the experimental error, microhardness measurements were performed by the same operator and consecutively along the same period of time.

Ultra-microindentation experiments were performed in a Nanotest-MicroMaterials equipment using a Berkovich indenter and a load of 30 mN. The hardness and elastic modulus calculations were done taking account of the Oliver & Pharr method [15]. To determine the Young's modulus, Poisson's coefficients of 0.07 for the tip and of 0.32 for the Ti-base alloy were used [16].

3. Results

Blasting of the alloy causes a severe deformation of the surface leaving a number of irregular protrusions and intrusions with sharp ridges, forming at some various places crack-like defects. The surface aspect is illustrated in Fig. 1 for both types of specimens. Examination of the surfaces reveals the presence of dark zones containing large particles, often broken, of heterogeneous size. X-ray mapping confirm they are Al-rich oxides, obviously remnants of the jet of particles used for blasting. A transfer of the blasting material onto the metal surface is usually reported [5,7,17]. From the analysis of the imprints in representative SEM images it follows that shape of the grit particles used to blast BL1and BL2 specimens might have been different. Grits used to process BL1 specimens are likely particles with blocky and angular shapes, producing greater cutting action, whereas those used to process BL2 specimens seem to be mostly rounded.

Surface deformation also induces a roughness increase (Ra) from 0.07 μm in the as-polished condition to about 1.7 and 0.53 μm for the BL1 and BL2 specimens, respectively. Relevant for the present work is that roughness increase is accompanied with an increase in the compressive residual stresses. Measurements obtained by synchrotron radiation indicate a gradient with maximum values close to the blasted surface of about 700 and 500 MPa for the BL1 and BL2 specimens, respectively [7].

Cross sectional examinations were performed by using backscattered electron images obtained on fresh polished surfaces. Operating at low voltages it is possible to obtain images where contrast results from differences in the average atomic number but also due to differences in the grain orientation. Fig. 2 shows representative images of the sub-surface blasted zones for the BL1, Fig.2a, and BL2, Fig.2b, specimens. Both images reveal the typical biphasic structure consisting of discontinuous bright zones (β-phase) into a dark matrix (α-phase). For the BL1 specimen, Fig. 2a, three different zones has been observed. Beneath the surface, a severely deformed zone, about 2-3 μm thick, with an ultrafine grained structure is observed. Next zone, about 8 to 11 μm thick, reveals a gradual increase of the grain size for the α- phase. Changes in the morphology of the β-phase clearly indicate that this zone was also severely deformed. Following this zone, modifications of the microstructure in terms of grain size and morphology, with regards to that of the sample interior, were not observed. In the case of the BL2 specimen, Fig. 2b, the severe deformation is confined to a thinner zone of about 5 μm in thickness.

Microhardness measurements were performed following different strategies along perpendicular and parallel lines at the possible closest distance to the blasted surface, i.e. two times the diagonal of the hardness imprint. Although the scattering of results was large, a clear indication of a sub-surface work hardening was not found. For illustrative purposes, Table 1 shows average hardness values obtained along a line parallel to the blasted surface, located at a depth of about 30 μm, and at the interior of the specimen, far away from the blasted affected zone. As it can be seen, hardness of BL1 specimen near to the surface and at the unblasted affected zone is similar. BL2 specimen, however, shows lower average values of hardness close to the surface. The standard deviation values at the surface and at the sample interior, however, gives not statistical meaning to such difference.

4. Discussion

Grit blasting of Ti6Al4V causes a severe deformation of the surface that is manifested by a change in the surface topography, from polished to randomly rough surface, and a subsurface refinement of the microstructure. Blasted specimens were supplied by different manufacturers. Thus, differences in roughness between BL1 (1.7 μm) and BL2 (0.53 μm) specimens, with regards to the as-polished condition (0.07μm), could be among others related to differences in the thermo mechanical route used to process the alloy, which is known to play an important role in further mechanical and fatigue behaviours [18,19]. Certificate analysis declares that both types of specimens were removed from hot rolled bars annealed at about 700ºC. Thermal cycling must have been nearly identical since microstructure of the alloys and their microhardness in the non-blasted affected zone is similar (Table 1).

Other factors influencing roughness concern the grit particles (nature, morphology, size distribution), blasting conditions (pressure, incidence angle, distance, time), and abrasive recycling. Moreover, size distribution of the grit particles might have been different since blasted disks were provided by different sources. Differences in roughness between BL1 and BL2 specimens could be explained as a combination of all factors referred before. In principle, the larger particle diameter of the grit used to process the BL2 specimens should have induced a larger roughness, which is not the case. A systematic analysis of the individual effect of the processing parameters on the morphological and microstructural features induced by blasting is not possible since most of them are slightly different or simply were not carefully controlled during processing.

Here it is worth noting that this work was aimed to understand the reasons behind the decrease in the fatigue strength of grit blasted Ti6Al4V alloys. From the practical point of view the blasted disks provide two surfaces with different roughness. In a previous study it has been shown that the maxima compressive residual stresses of BL1 and BL2 specimens are different (700 and 500 MPa, respectively) [7], which denotes differences in the cold-working degree in the subsurface layer during blasting. This feature makes both types of specimens appropriated to correlate changes in the microstructure and subsurface hardening. For the analysis it was taken into consideration that blasting of cp Ti with Al_2O_3 [11] or SiO_2 [4] particles, however, improves the fatigue life, irrespectively of its microstructure [11]. The key features pointed out in the literature as affecting the endurance limit of Ti6Al4V are the surface compressive residual stress state, the microstructure near to the surface, the surface material texture and the presence of stress raisers at the blasted surface [4,6,10]. The presence of microcracks at the surface and the pronounced stress concentration in the vicinity of the particles, which remain embedded onto the surface, have also been pointed out as responsible for the loss of fatigue strength. It has been argued that superficial cracks due to grit blasting have been observed in Ti6Al4V but not in cp titanium, likely due to the higher ductility [20]. Other authors, however, have also observed such surface defects on blasted titanium, being the net effect of grit blasting for this material beneficial [11]. Therefore, the negative influence of stress raisers associated to the presence of microcracks, pits, or embedded ceramics particles cannot be discarded, but it not seem to be the only reason for the decrease in the fatigue limit of the blasted Ti6Al4V.

An interesting effect induced by the severe plastic deformation is work hardening due to the increased near-surface dislocation density at the grit blasted affected zone [9]. Hardness increase in the near surface of about 60% for cp Ti [4,11] and 75% for austenitic stainless steel 316 L [13] have been reported. Hardness decreased with increasing depth, remaining nearly constant after about 60 and 200 μm of the surface, respectively.

Results of the present work, however, have shown a negligible net effect of grit blasting on the near surface hardening of Ti6Al4V. As can be seen in Table 1, the average hardness value close to the blasted surface is similar (BL1) or even inferior (BL2) to that of the bulk. The formulation of a net subsurface softening for the BL2 specimen is however not possible when considering the standard deviation. A question still arises about why the average hardness value at the subsurface of the BL2 specimen is lower than that for the BL1 specimen. Here it is worth to remark that pre-existing compressive residual stresses at the subsurface zone will tend to decrease the size of the indentation after removing the load, giving a nominal higher hardness value [21,22]. Measurements of residual stresses by synchrotron radiation of the materials investigated in the present work determined the existence of a gradient in the compressive stresses [7]. The maximum values, measured at about 20 μm of the blasted surface, were 700 and 500 MPa for the BL1 and BL2 specimens, respectively. The higher level of pre-existing residual stresses for the BL1 specimen would cause a heavier contribution on the nominal hardness, thus somewhat lower differences in the real hardness could be expected.

Such residual stress effect on hardness would not occur when using instrumented indentation experiments since hardness is determined at the maximum load, before the unloaded stage. To check this effect, ultra-micro hardness tests were performed along perpendicular lines to the blasted surface. The relevant results are presented in Figure 3. As can be seen, despite the relative large scattering, hardness and Young's modulus remain practically constant with increasing depth for both types of specimens.

The negligible effect of grit blasting on the near surface hardening can be related with the low value of the strain hardening exponent (about 0.048) [23], which contrasts with the higher values determined for cp Ti (about 0.5) [23] and 316 L alloy (about 0.41) [24]. A question still arises about the absence of hardening despite the refinement of the microstructure observed in the subsurface blasted zone. According to the Considère criterion the lack of hardening mechanisms originates plastic instabilities that yield highly-localized deformation, which is very effective in grain refinement but contributes little to strength [25].

Another feature that must be taken into consideration is the potential induced softening associated with the fatigue process at the surface layer. Similarly to the shot-peening process [26], blasting pressure can be described as the stress amplitude, and the exposure time, as the number of cycles. Previous results have shown that whereas cp Ti hardens [23], Ti6Al4V experiences an opposite behaviour [20]. These results, however, are not conclusive. For instance, Leinenbach and Eifler observed pronounced cyclic softening and subsequent hardening for cp-Ti grade 2 [27]. The same authors observed both cyclic softening and subsequent hardening on two different batches of Ti-6Al-4V, but with much smaller plastic strain amplitudes [28]. Therefore, the contribution of the cyclic plastic deformation to the net hardness value remains uncertain.

Implications of the absence of hardening at the surface on the loss of fatigue strength are next analysed. On one hand, the compressive residual stresses at the surface play a beneficial role by lowering the effective tensile stress during fatigue [9,29], being the net effect similar to the increase in strength associated with hardening. Since residual stresses have been observed to decay with increasing the number of fatigue cycles [26], the absence of hardening will highlight the residual stresses relaxation. On the other hand, this feature could also explain why fatigue cracks initiate mainly at the surface, in the vicinity of the alumina particles [6], rather than at the sub-surface as it was observed for cp blasted Ti, for which sub-surface work hardening was observed [4]. It seems that in the absence of subsurface hardening in the grit blasted Ti6Al4V alloy, the beneficial effect of the compressive residual stresses at the earlier stages of the fatigue process is offset by the presence of microcrack-like defects, pits, and embedded particles all them acting as severe notches

A controversial point is that shot-peening of Ti6Al4V slightly increases the fatigue limit from about 65% σ_y to 71% σ_y of the as-received material [30]. The benefits of shot-peening were attributed to the development of compressive residual stresses. The lower roughness and the absence of microcraks-like defects at the surface provides the alloy with additional advantages in comparison to the blasted materials. Recently it has been also reported that fine-particle bombarding of Ti6Al4V alloy with SiC particles (diameter 75 μm) or steel particles (diameter 69 μm) followed by Al_2O_3 particles (diameter 61 μm) increased up to about 25% the fatigue strength in the absence of hardening at the subsurface layer [8]. Reasons for this improvement in the fatigue strength remains uncertain since relevant data like roughness and microstructural analysis of the deformed affected zone are not shown.

5. Conclusions

- Blasting of Ti6Al4V alloy produces an increase in roughness associated to the severe plastic deformation of the surface. Such deformation, however, does not cause any evident hardening at the sub-surface zone, which is associated to the low hardening coefficient of the alloy. The lack of hardening mechanisms originates plastic instabilities that yield highly-localized deformation, which is very effective in grain refinement but contributes little to strength.

- This finding could be playing a critical role in the decrease of the fatigue strength reported by other authors. In the absence of subsurface hardening for the grit blasted Ti6Al4V alloy, the beneficial effect of the compressive residual stresses at the earlier stages of the fatigue process would be offset by the presence of microcrack-like defects, pits, and embedded particles all them acting as severe notches.

Acknowledgements

The authors thank BIOMET-IQL and SURGIVAL S.A. for the surface modification of the specimens and financial support to Ministerio de Educación y Ciencia, Spain. (MAT2006-12948-C04-01) and Fundación Mutua Madrileña (Spain). Dra M.M. thanks to the Ministerio de Educación y Ciencia the "Juan de la Cierva" grant. The CIBER-BBN of Bioingeniería, Biomateriales y Nanomedicina is supported by the ISCIII.

Reference list

[1] A. Wennerberg, T. Albrektsson, B. Andersson, Int. J. Oral. Maxillofac. Implants 11 (1996) 38.

[2] V.M. Goldberg, S. Stevenson, J. Feighan, D. Davy, Clin. Orthop. Relat. Res. 319 (1995) 122.

[3] C. Aparicio, F.J. Gil, U. Thams, F. Muñoz, A. Padrós, J.A. Planell, Key Eng. Mater. 254-256 (2004) 737.

[4] X.P. Jiang, X.Y. Wang, J.X. Li, D.Y. Li, C.-S. Man, M.J. Shepard, T. Zhai, Mater. Sci. Eng. A 429 (2006) 30.

[5] C. Aparicio, F.J. Gil, C. Fonseca, M.Barbosa, J.A. Planell, Biomaterials 24 (2003) 263.

[6] C. Leinenbach, D. Eifler, Biomaterials 27 (2006) 1200.

[7] M. Multigner, P. Fernández-Castrillo, S. Ferreira-Barragán, G. González-Doncel, J.L. González-Carrasco, Rev. Metal. Madrid 2008 in press.

[8] T. Morita, T. Ohtomo, C. Kagaya, N. Tsuji, S. Tanaka, T. Miyasaka, Ti-Technology, Proc. 11th World Conference of Titanium (JIMIC5), Vol. II (2007) p 1659.

[9] L. Wagner, Mater. Sci. Eng. A263 (1999) 210.

[10] M. Baleani, M. Viceconti, A. Toni, Artif. Org. 24 (2000) 296.

[11] F.J. Gil, J.A. Planell, A. Padrós, C. Aparicio, Dent. Mater. 23 (4) (2007) 486.

[12] L. Wagner and G. Lüetjering, Influence of Shot Peening on the Fatigue behaviour of titanium alloys. ICSP-1, (Niku-Lari, eds) France, (1981) 453.

[13] M. Multigner, E. Frutos, J. L. González-Carrasco, J.A. Jiménez, P. Marín, J. Ibáñez, Mater. Sci. Eng. C, Accepted for publication (2008)

[14] M. Multigner, P. Fernández-Castrillo, S. Ferreira, G. González-Doncel, J. L. González-Carrasco, In XXX Congreso de la Sociedad Ibérica de Biomecánica y Biomateriales, 15-17 Nov. 2007, Madrid.

[15] W. C. Oliver and G. M. Pharr, J. Mater. Res. 7 (6) (1992) 1564.

[16] Titanium-A technical guide, Ed M. J. Donachie, Jr, ASM International, Materials Park (2000) 118.

[17] L.Saldaña, V.Barranco, J.L. González-Carrasco, M. Rodríguez, L.Munuera, N.Vilaboa, J. Biomed. Mater. Res. 81A (2) (2007) 334.

[18] G.Lütjering, Mater. Sci. Eng. A243 (1998) 32.

[19] J. Mueller, H.J. Rack, L. Wagner, Effect of Supra- and Subtransus Heat Treatment on Fatigue Performance of Ti-6Al-4V, Ti-2007: Science and Technology, vol. 1, pp 383-386, The Japan Institute of Metals (2007)

[20] E. Conforto, B.-O Aronsson, A. Salito, C. Crestou, D. Caillard, Mater. Sci. Eng. C 24 (2004) 611.

[21] T. R. Simes, S.G. Mellor, D.A. Hills, J. Strain Anal. 19 (2) (1984) 135.

[22] L.Y Chen, Q.Ge, S.Qu and J.Z. Jiang, Scrip. Mater. 59 (2008) 1210.

[23] Chr. Boller, T. Seeger, Materials Data for Cyclic Loading. Part. D: Aluminium and Titanium Alloys. Materials Science Monograph, 42 D. Elsevier, Amsterdam, (1987) 127.

[24] T.S. Byun, K. Farrel, E.H. Lee, J.D. Hunn, L.K. Mansur, J. Nuclear Mater. 298 (2001) 269.

[25] Y.L. Hao, S.J. Li, S. Y. Sun, C.Y. Zheng, Q.M. Hu, and R. Yang, Applied Physics Letter 87, (2005) 091906-1.

[26] L. Wagner and G. Lüetjering, Influence of the Shot Peening Parameters on the Surface Layer Properties and the Fatigue Life of Ti-6Al-4V, ICSP-2, G.P. Balear and H.O. Fuchs (eds), Chicago, IL , USA (1984) 195.

[27] C. Leinenbach, D. Eifler, Z. Metallk. 95(6) (2004) 535.

[28] C. Leinenbach, B. Schwilling, D. Eifler, Mater. Sci. Eng. C 25 (2005) 321.

[29] H. Gray, L. Wagner, G. Lütjering, Influence of Shot Peening Induced Surface Roughness, Residual Macrostresses and Dislocations Density on the Elevated Temperatures HCF-Properties of Ti alloys, ICSP -3, (H. Wohlfahrt, R. Kopp, O. Vöhringer Eds), 1987, Garmisch-Parterkirchen, Germany, 447.

[30] X.P. Jiang, C.-S. Man, M.J. Shepard, T. Zhai, Mater. Sci. Eng. A 468-470 (2007) 137.

LEGENDES OF THE FIGURES

Fig. 1. Backscattered electron images of the surface of grit blasted specimens. A) BL1 and B) BL2.

Fig. 2. Backscattered electron images corresponding to a transverse section of the A) BL1 and B) BL2 specimens.

Fig. 3. Young's modulus and Berkovich hardness under load of 30 mN as a function of depth from the blasted surface for the BL1 and BL2 specimens.

Table 1. Microhardness values (GPa) obtained with a maximum load of 98 mN at places close to the surface and interior of the specimens.

Specimen	30 μm from the surface	1000 μm from the surface
BL1	3,95± 0,21	3,98 ± 0,23
BL2	3,59 ± 0,35	3,94 ± 0,35

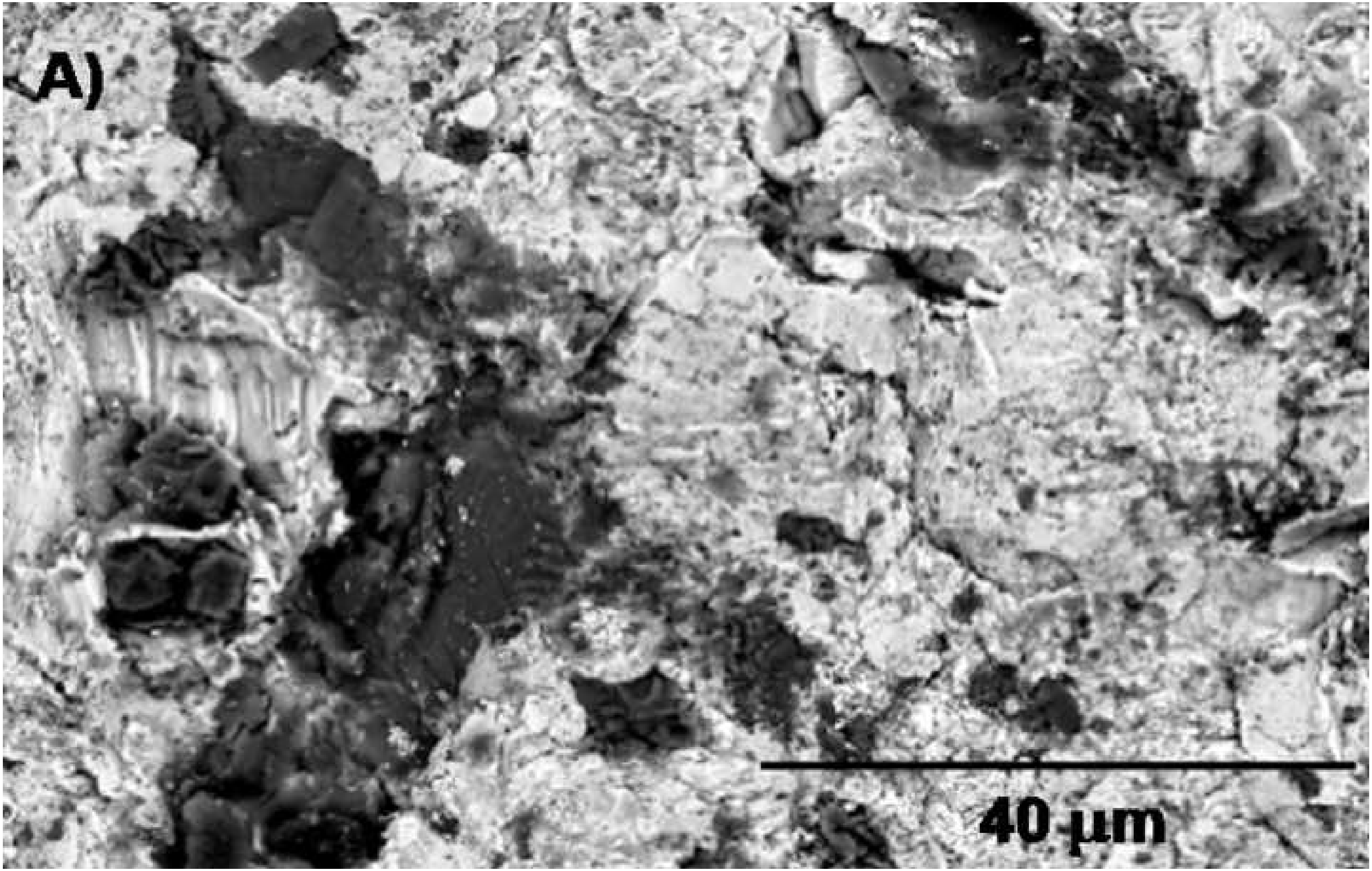
A)
40 µm

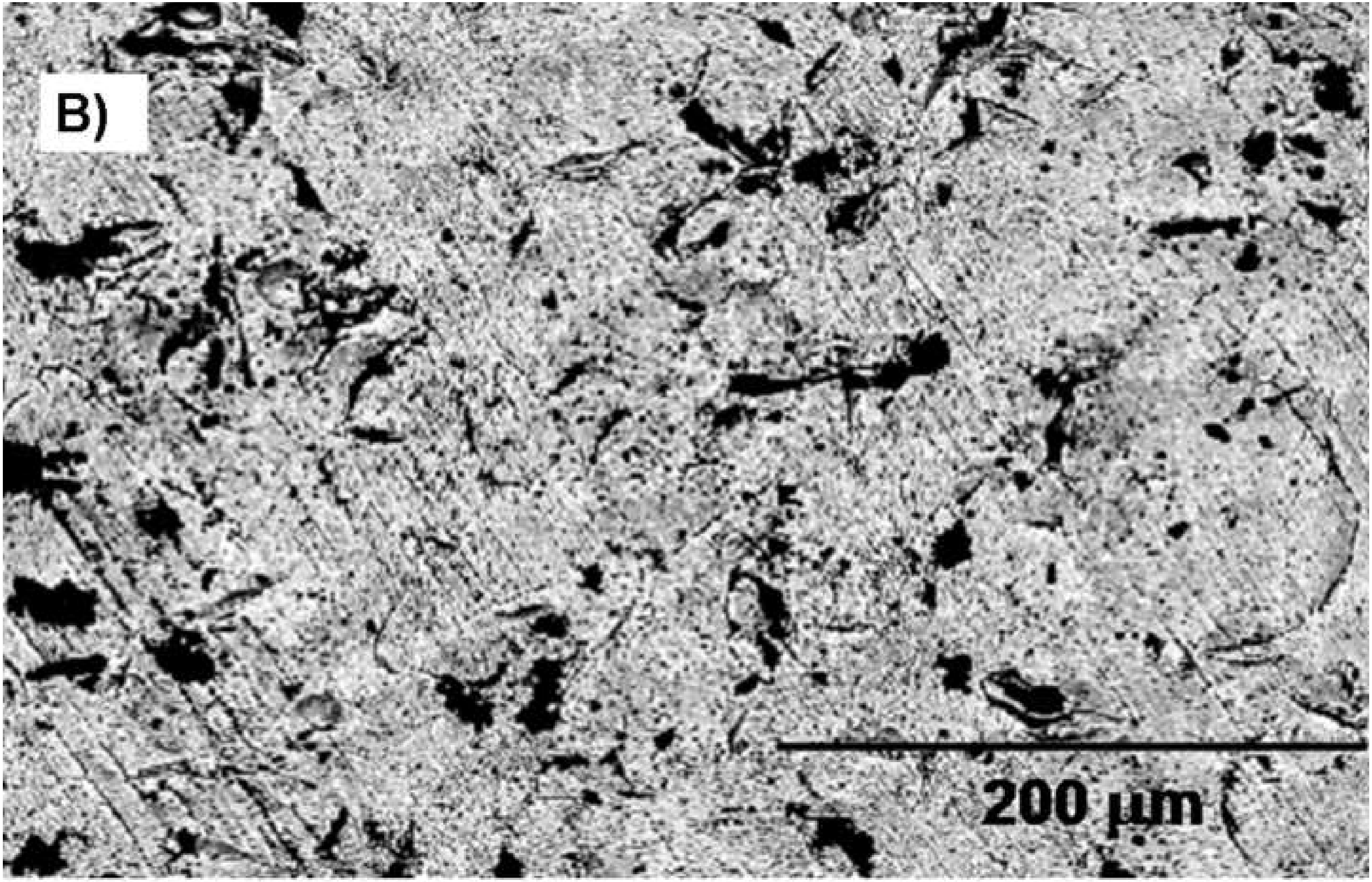
B)
200 µm

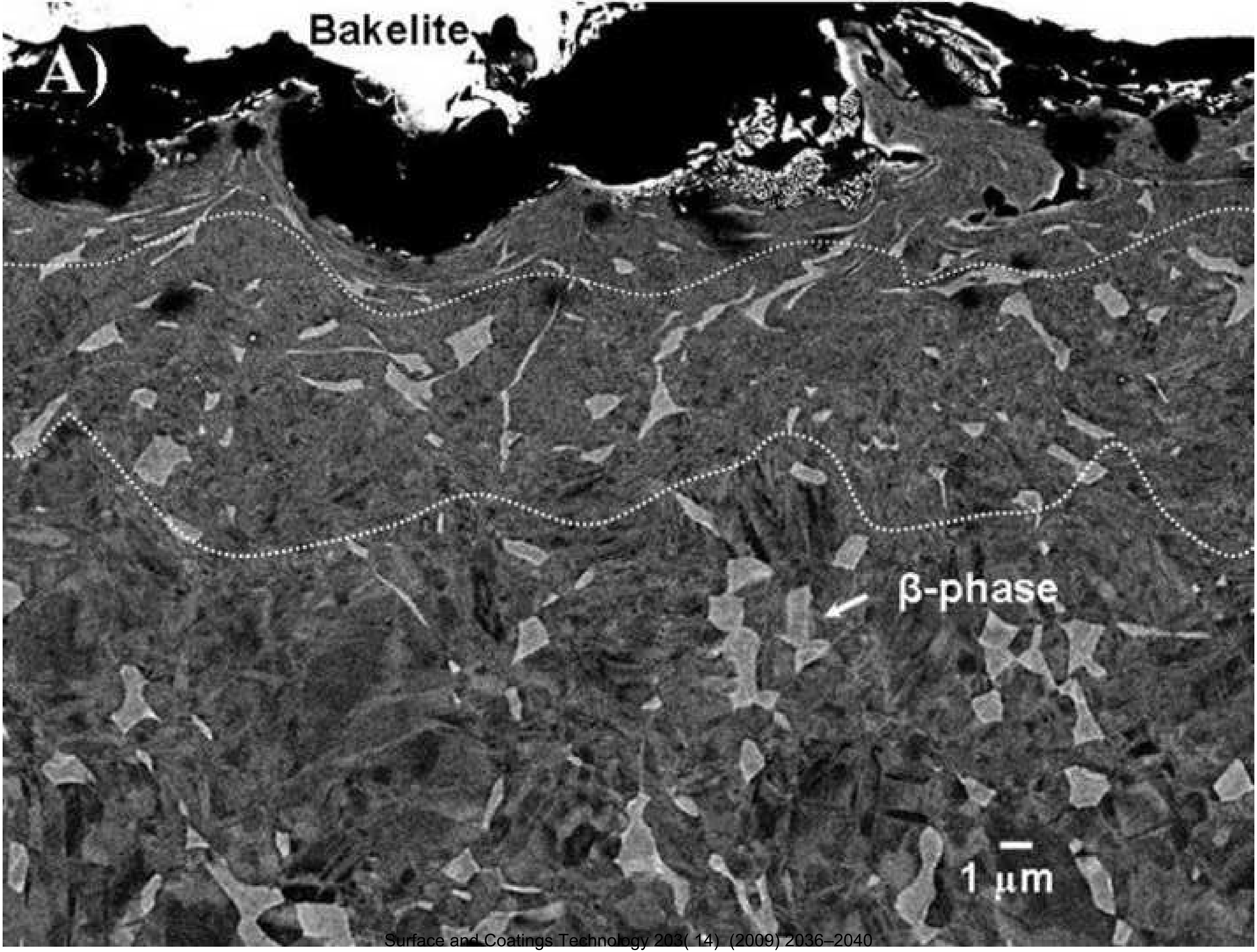
A)
Bakelite
β-phase
1 μm

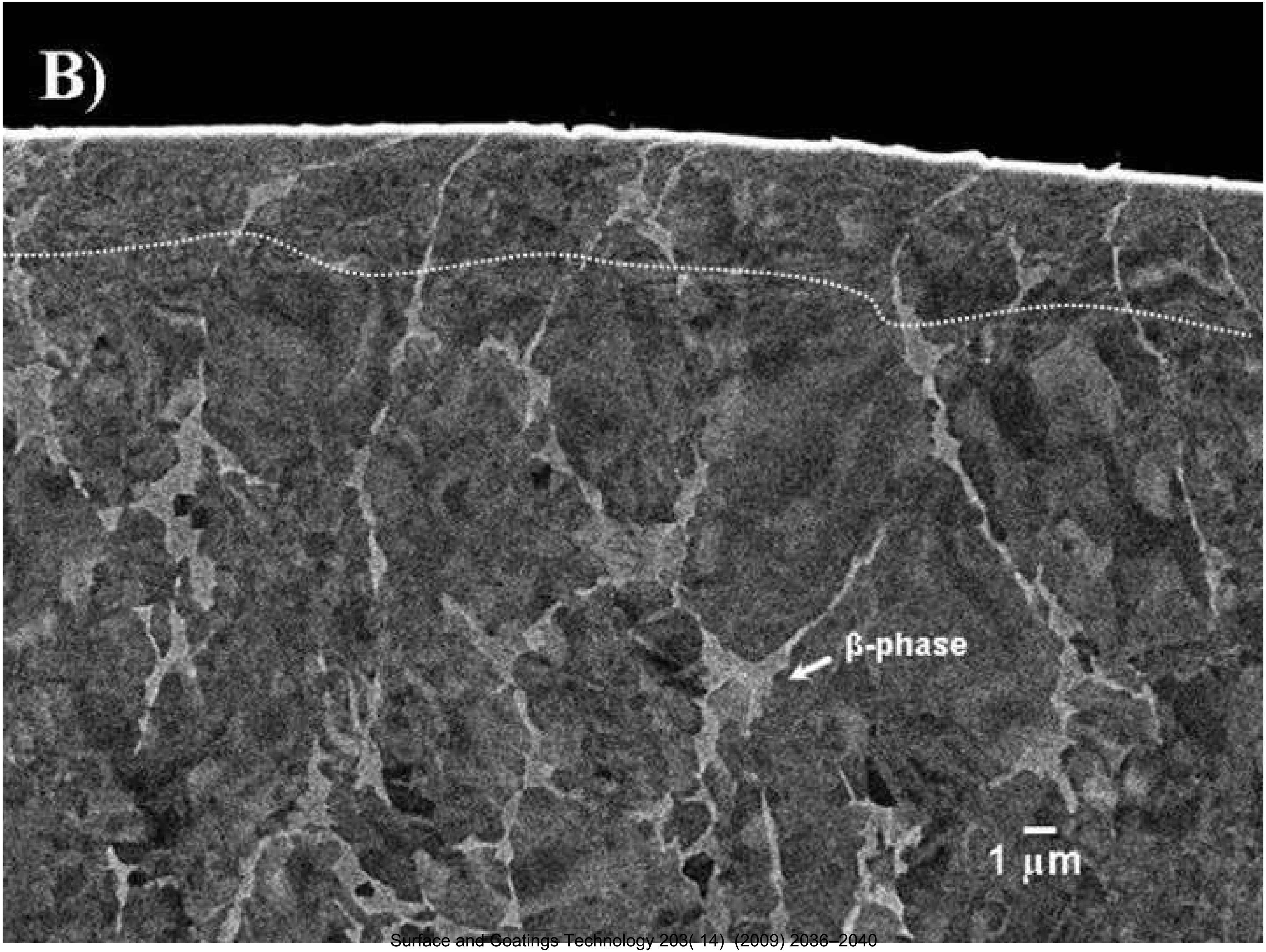
B)
β-phase
1 μm

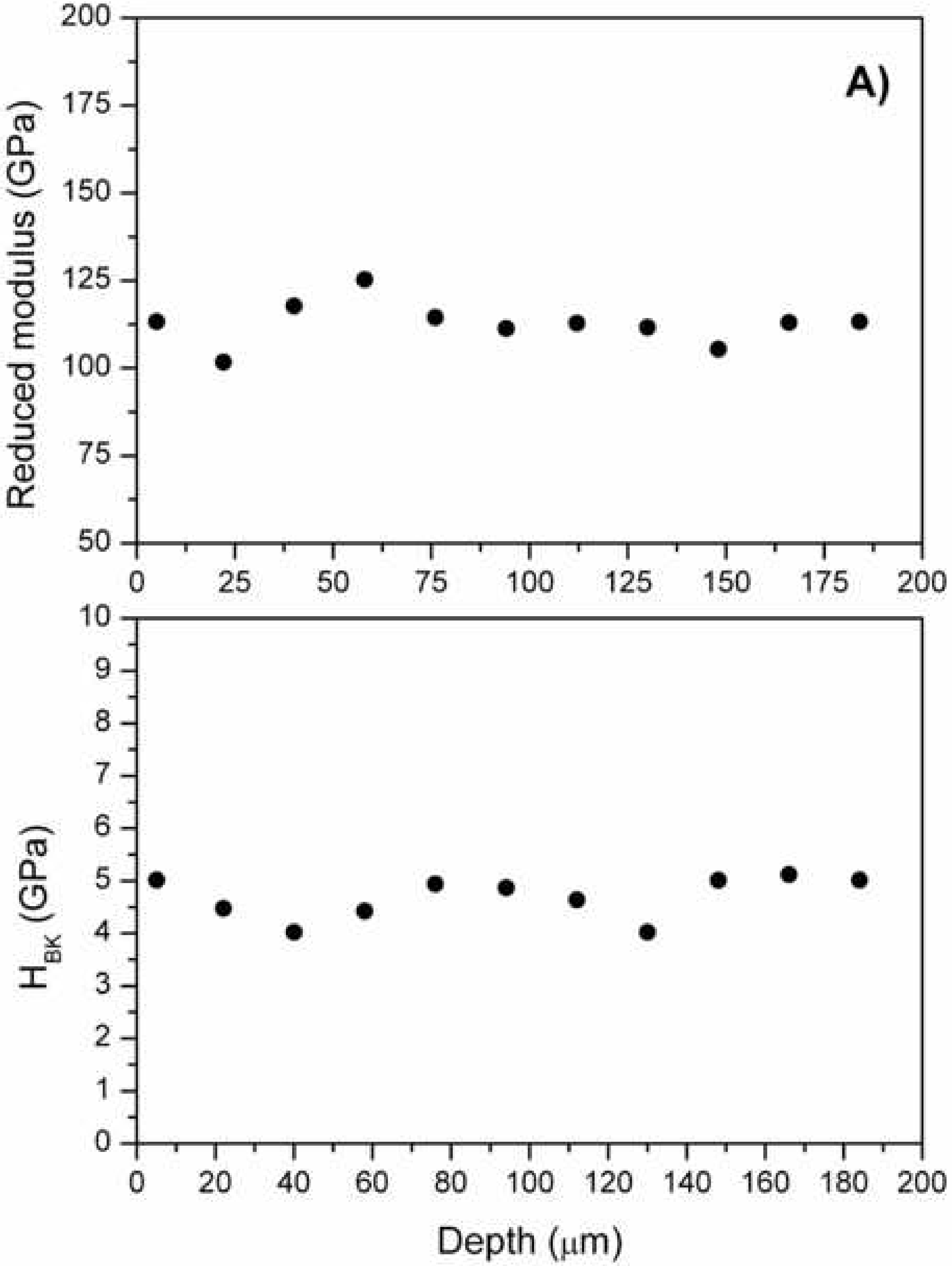
A)
Reduced modulus (GPa)
200
175
150
125
100
75
50
0
25
50
75
100
125
150
175
200
H$_{BK}$ (GPa)
10
9
8
7
6
5
4
3
2
1
0
0
20
40
60
80
100
120
140
160
180
200
Depth (μm)

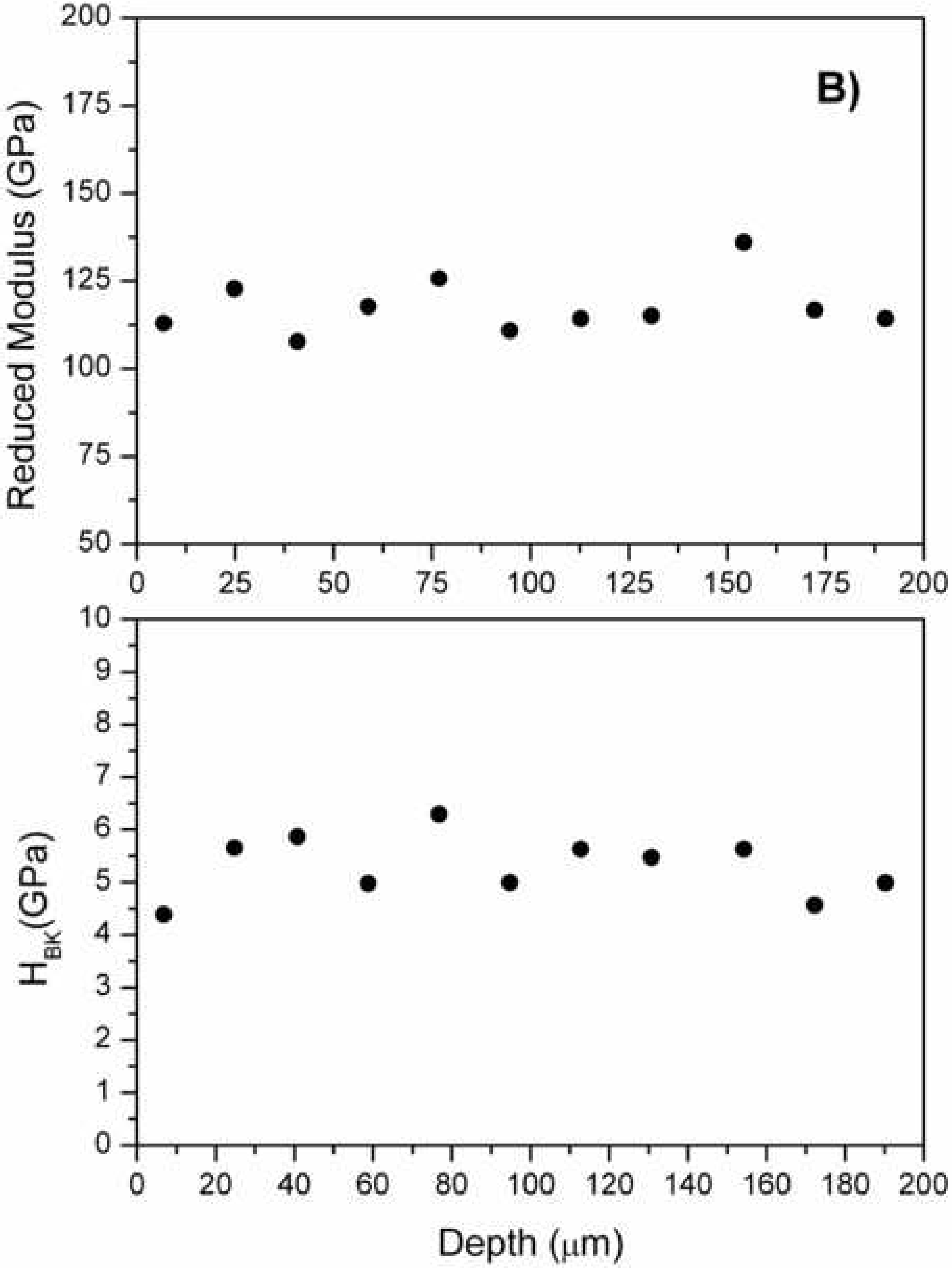
B)
Reduced Modulus (GPa)
200
175
150
125
100
75
50
0
25
50
75
100
125
150
175
200
H_{BK}(GPa)
10
9
8
7
6
5
4
3
2
1
0
0
20
40
60
80
100
120
140
160
180
200
Depth (μm)